Nonlinear Saturation of Topographically Forced Rossby Waves in a Barotropic Model

CONSTANTINE GIANNITSIS* AND RICHARD S. LINDZEN

Program for Atmospheres, Oceans, and Climate, Massachusetts Institute of Technology, Cambridge, Massachusetts

(Manuscript received 17 July 2000, in final form 20 March 2001)

ABSTRACT

A quasigeostrophic barotropic model is used to examine the nonlinear saturation of forced Rossby waves and the role of wave–wave interactions in limiting the wave growth. A simple mechanism, based on wave interference, is used to produce strong transient eddy growth and an analytical linear solution for the flow evolution is used as a starting point. Given the rigid upper bound on wave growth, set by the potential enstrophy conservation principle, the linear solution is bound to break down at high forcing amplitudes. An analytical quasi-linear solution, which guarantees potential enstrophy conservation, is formulated and its domain of validity is examined with a numerical nonlinear model. The nonlinear flow evolution is shown to bear strong similarity to the analytical quasi-linear solution and wave–mean flow interactions are found to be always sufficient to limit wave growth. The saturation of the forced disturbances is shown to come through the deceleration of the mean flow and the modification of the topographic vorticity forcing. Overall, wave–wave interactions prove not to be important in the saturation process in the examples considered. While the authors consider the implications of this result for the observationally more relevant case of vertically propagating Rossby waves, explicit calculations are clearly called for.

1. Introduction

The issue of propagation of planetary waves into the stratosphere has long been central to the stratospheric dynamics literature due to the importance of the effects of eddies on the mean circulation and the distribution of ozone, as well as other chemical species. An important question, regarding the vertical propagation of such disturbances, was first posed by Charney and Drazin (1961). Noting that the transport of energy by propagating planetary waves could lead to strong changes in the thermal structure of the thermosphere, where the density of air is small, Charney and Drazin (1961) tried to find a dynamical explanation for the apparent lack of deep wave penetration. Examining simple basic states, representative of the zonal mean flow at different seasons, they found that linear propagation alone seemed capable of blocking the propagation of planetary-scale anomalies to high altitudes.

Complementary to the results of Charney and Drazin (1961), the sphericity of the earth's geometry (Karoly and Hoskins 1982) and thermal damping (Dickinson 1969) were also shown to act in the direction of preventing strong vertical wave propagation. However, it is not clear whether linear dynamics alone are sufficient to resolve the problem, as large wave growth is often observed in the winter stratosphere, leading to strongly nonlinear phenomena (McIntyre and Palmer 1983). A rather clear answer to the original concern of Charney and Drazin (1961) was, however, given by Lindzen and Schoeberl (1982). Using concepts of quasigeostrophic theory Lindzen and Schoeberl (1982) argued that potential vorticity and potential enstrophy conservation would naturally limit wave amplitudes, independently of the details of the flow dynamics. In simple terms, Lindzen and Schoeberl (1982) argued that the limitation of wave amplitudes by the amount of potential enstrophy initially available in the zonal mean flow was sufficient to prevent the formation of a terrestrial corona.

While Lindzen and Schoeberl (1982), as well as related studies (Schoeberl 1983), hint at the existence of a saturation limit for vertically propagating waves, they were not concerned with the specific mechanism through which saturation could be achieved. Garcia (1991), on the other hand, put forth a hypothesis that saturation of vertically propagating waves occurred qualitatively similarly to that of gravity waves, where the wave breaking process is believed to dissipate wave activity, preventing growth above a certain amplitude (Lindzen 1981). In the mechanism proposed by Garcia (1991), barotropic instabilities were assumed to be an important part of the nonlinear saturation process, leading to a cascade of ''excess'' potential enstrophy to small scales where dissipation can come into play. While the description of Garcia (1991) was based on physically plausible mechanisms, and the previous findings of

* Deceased.

Corresponding author address: Richard S. Lindzen, 54-1720, Massachusetts Institute of Technology, Cambridge, MA 02139.
E-mail: rlindzen@mit.edu

Haynes (1985) and Killworth and McIntyre (1985) concerning the instability of a nonlinear Rossby wave critical layer, it consisted of an ad hoc assumption about the dynamics.

Altogether, since the pioneering work of Warn and Warn (1978) and Stewartson (1978), a lot of emphasis has been put on the phenomenology of Rossby wave breaking in the stratosphere (McIntyre and Palmer 1983, 1985; Polvani and Plumb 1992), the assumption being that some mechanism similar to that described in Garcia (1991) would lead to saturation of the propagating disturbance. Interestingly, a significant number of studies have relied on one-layer models forced by a bottom topography (Juckes and McIntyre 1987; Polvani et al. 1995), exploiting the quasi-two-dimensional nature of midlatitude dynamics. While such models have the horizontal resolution necessary to capture the full spectrum of scales resulting from the nonlinear flow evolution, they do not take into account the possibility that the propagating wave might be prevented from reaching the upper levels of the stratosphere and from attaining high amplitudes.

Nonetheless, in the present study we also approach the issue of wave saturation using a simple barotropic quasigeostrophic model. Given the points raised above, our goal is not to simulate the vertical propagation of a wave, but rather to use the barotropic model as a tool in exploring the dynamics. As the internal dynamics of the barotropic flow can alter the ''effective'' topographic forcing and affect the growth of the forced disturbance, a connection to the three-dimensional case, where the growth of a wave depends on its ability to propagate vertically, seems possible. Our present interest lies in understanding the mechanism through which wave saturation is achieved, and whether the enstrophy constraint proves relevant. We want to examine whether wave–mean flow interactions can limit sufficiently the amplitude of the eddy disturbance or whether strong wave–wave interactions are indispensible. Contrary to Polvani et al. (1995), our interest is specifically in looking at the feedback between the interior dynamics and the forcing of the large-scale disturbance from the bottom boundary. While it is well understood that the barotropic model cannot fully capture the behavior of the three-dimensional flow, the strong similarity of the barotropic potential vorticity equation to the formulation for a three-dimensional flow allows for at least a zero-order connection.

2. Wave growth through interference

The model of Lindzen et al. (1982) provides a simple mechanism for obtaining transient wave growth in a barotropic model through the interference between a topographically forced wave and a free Rossby wave with the same spatial characteristics as the forced wave. Initial total wave amplitude can be set to zero by requiring that the free Rossby wave have the same amplitude as the forced wave, but the opposite phase. However, the propagation of the free wave will eventually lead to positive interference and growth of the total amplitude. Such an approach to wave growth has the advantage of conserving potential enstrophy, contrary to the usual practice of gradually introducing a topographic anomaly, which acts as a potential enstrophy source.

It will be helpful to our subsequent discussion to briefly review some specific results from Lindzen et al. (1982). They use a barotropic beta-plane channel model with a uniform zonal flow, U_0, over topography given by $h'(x, y) = h \sin(kx) \sin(ly)$. The initial flow is taken to be purely zonal, which requires a free Rossby wave of amplitude equal to the forced wave and opposite phase. The superposition of the two waves leads to periodic growth and decay of the total wave field. At second order in a Rossby number expansion, the free wave interacts with the topography to produce vacillations in the mean flow consistent with conservation of total kinetic energy. The solution obtained by Lindzen et al. (1982) is briefly as follows:

$$\frac{\partial}{\partial t}\nabla^2\Psi + J(\Psi, \nabla^2\Psi + \beta y) = -J\left(\Psi, \frac{f_0}{H}h'\right), \quad (1)$$

$$\Psi = \Psi_0 + \epsilon\Psi_1 + \epsilon^2\Psi_2 + \cdots, \quad (2)$$

$$\Psi_0 = -U_0 y, \quad (3a)$$

$$\Psi_1 = A_1[\sin(kx) - \sin(kx - kct)] \sin(ly), \quad (3b)$$

$$\Psi_2 = A_1A_2\left[y - \frac{1}{2l}\sin(2ly)\right][1 - \cos(kct)], \quad (3c)$$

$$A_1 = \frac{U_0}{c}\frac{1}{(k^2 - l^2)}\left(\frac{f_0}{H}h\right), \qquad A_2 = \frac{1}{4}\left(\frac{f_0}{H}h\right)\frac{1}{c}, \quad (4)$$

$$c = U_0 - \frac{\beta}{k^2 + l^2}. \quad (5)$$

3. Wave–mean flow interaction

The solution of Lindzen et al. (1982) predicts a linear dependence of the maximum superposition amplitude on the height of the topographic anomaly and places no limits on the growth of the waves. However, as the topographic forcing amplitude increases, one expects the linear prediction to lead to a contradiction with the potential enstrophy constraint. Given the conservation of potential enstrophy in the fully nonlinear system, the maximum amount of enstrophy the waves can draw from the mean flow is limited by the initial mean available potential enstrophy.[1] Therefore a breakdown of the

[1] Mean available potential enstrophy is defined as $1/L_y \int_y 1/2[\overline{q}(t) - q_0]^2\, dy$, where q_0 represents the average initial potential vorticity $1/L_y \int_y \overline{q}(0)\, dy$. Eddy growth can only be sustained as long as a background gradient of potential vorticity exists.

linear solution is expected at sufficiently high topographic forcing values.

Still, one can at least attempt a qualitative examination of the dynamics at the high-amplitude limit, using the solution of Lindzen et al. (1982). From the potential vorticity equation one can form a potential enstrophy budget, examining the evolution of the eddy enstrophy field separately from the zonal mean flow. Separating into terms denoting the wave–mean flow interactions versus nonlinear terms one has

$$\frac{\partial}{\partial t}\frac{\langle\overline{\zeta'^2}\rangle}{2} = \underbrace{\left\langle\overline{\zeta'\left[-v'\left(\beta + \frac{\partial\overline{\zeta}}{\partial y}\right)\right]}\right\rangle}_{C_1} + \underbrace{\left\langle\overline{\zeta'\left[-\overline{u}\frac{f_0}{H}\frac{\partial h'}{\partial x}\right]}\right\rangle}_{C_2} + \underbrace{\left\langle\overline{\zeta'\left[-J\left(\Psi', \frac{f_0}{H}h'\right)\right]}\right\rangle}_{C_3}, \tag{6}$$

where $\zeta = \nabla^2\Psi$, overbars denote zonal averages, angle brackets denote integration over latitudes, and primed quantities correspond to deviations from the zonal mean fields. For the linear solution of Lindzen et al. (1982) only the term C_2 is nonzero. The physical meaning of term C_2 is somewhat blurred, as it represents the correlation between the topographic forcing by the mean flow and the preexisting eddy vorticity field. For $\overline{u} = U_0$ positive perturbations in the potential vorticity field can be shown to grow as they propagate along the lee side of the topography and decay along the windward side, with the opposite being true for negative perturbations. Thus, for a westward propagating wave, the total eddy enstrophy experiences continuous growth during the propagation of the cyclonic (anticyclonic) vorticity centers from the topographic low (high) to the topographic high (low), and decays subsequently. As the topographic vorticity forcing $(-\overline{u}(f_0/H)(\partial h'/\partial x))$ remains constant, the wave enstrophy maximizes when the propagating disturbance phase locks with the topography.

Considering, however, the effect of wave drag on the mean flow, the possibility arises that the eddy enstrophy growth may be disrupted due to changes in the mean winds. For wave drag strong enough to produce zonal mean easterlies the topographic forcing term $(-\overline{u}(f_0/H)(\partial h'/\partial x))$ changes sign before the propagating disturbance assumes a perfect phase relationship with the topography, ''prematurely'' disrupting the eddy growth cycle. Thus the possibility arises that saturation of the wave growth might be achieved through a purely quasi-linear mechanism, without the involvement of stronger nonlinearities. Whether quasi-linear interactions are sufficient to prevent the violation of the potential enstrophy constraint in the high-amplitude limit is not, however, clear a priori.

4. Quasi-linear analytical solution

In the linear solution of Lindzen et al. (1982) the modification of the mean flow only affected the solution for the wave field to third order in the perturbation expansion. One can, however, reformulate the problem so as to get a ''quasi-linear'' system of equations, where the forcing of waves by the zonal mean flow and the effect of wave drag on the mean winds are taken into account simultaneously. Rambaldi and Flierl (1983) developed such a system of equations for a one-dimensional flow. Qualitatively the flow behavior is expected to be similar to the case of the two-dimensional channel, since in the latter propagation is limited to the zonal direction by the side walls. The original equations presented in Rambaldi and Flierl (1983) did not involve any linearizations. Here, however, to obtain analytical solutions, a linearized version of the quasi-linear system is used and a perturbation expansion method is followed.

The zeroth-order solution for the flow in Rambaldi and Flierl (1983) consists of a zonal mean velocity U_0^*, a topographic anomaly $h' = h\sin(kx)$, and a stationary wave $\Psi_0^* = A_0^*\sin(kx)$, where

$$A_0^* = \frac{U_0^*}{c^*}\frac{1}{k^2}\left(\frac{f_0}{H}h\right). \tag{7}$$

To first order one obtains a system of two equations; the first one represents the effect of wave drag onto the zonal mean velocity. The second is derived directly from the potential vorticity equation, linearized around the zero-order basic state, and represents the time evolution of nonzonal perturbations:

$$\frac{\partial U_1^*}{\partial t} = -\overline{\Psi_1^*\frac{\partial}{\partial x}\left(\frac{f_0}{H}h'\right)}, \tag{8a}$$

$$\frac{\partial}{\partial t}\left(\frac{\partial^2\Psi_1^*}{\partial x^2}\right) + U_0^*\frac{\partial}{\partial x}\left(\frac{\partial^2\Psi_1^*}{\partial x^2}\right) + \beta\frac{\partial\Psi_1^*}{\partial x} = -U_1^*\frac{\partial}{\partial x}\left(\frac{f_0}{H}h' + \frac{\partial^2\Psi_0^*}{\partial x^2}\right). \tag{8b}$$

Substituting the expressions for h', Ψ_0^* into the equations above, and expressing Ψ_1^* as $\Psi_1^* = A_1^*(t)\sin(kx) + B_1^*(t)\cos(kx)$, one obtains

$$\frac{dU_1^*}{dt} = -\frac{1}{2}k\frac{f_0}{H}hB_1^* \tag{9a}$$

$$\frac{dA_1^*}{dt} = k\left(U_0^* - \frac{\beta}{k^2}\right)B_1^* \tag{9b}$$

$$\frac{dB_1^*}{dt} = -k\left(U_0^* - \frac{\beta}{k^2}\right)A_1^* + k\left(-A_0^* + \frac{1}{k^2}\frac{f_0}{H}h\right)U_1^*. \tag{9c}$$

Rambaldi and Flierl (1983), using the original system of equations, searched for nonlinear equilibrium points of the flow. Prescribing the total kinetic energy and potential enstrophy and leaving U^* (the total zonal mean zonal flow) as a free variable, three different possible equilibrium solutions were found to exist. Two stable equilibria were identified, corresponding to subcritical and supercritical flows ($U^* - \beta/k^2 < 0$ and $U^* - \beta/k^2 > 0$, respectively), separated by an unstable point representing the form drag instability regime discussed by Charney and DeVore (1979) ($U^* - \beta/k^2 \simeq 0$). Focusing on the behavior of the flow in the vicinity of the stable equilibria, perturbations around them were found to have eigenfrequencies that depended not only on the values of U_0^*, β, and k^2, but also on the amplitude of the topography and the equilibrium stationary wave:

$$\omega_1^* = \sqrt{\left(U_1^* - \frac{\beta}{k^2}\right)^2 k^2 + \frac{1}{2}\left(\frac{f_0}{H}h\right)\left(-A_0^* + \frac{1}{k^2}\frac{f_0}{H}h\right)k^2}. \tag{10}$$

This last result represents a very important difference from the linear solution of Lindzen et al. (1982), where the vacillation frequency is determined by the speed of free waves on the zonally symmetric basic state. In the quasi-linear equations one cannot think in terms of free traveling waves. Rather, as perturbations in the zonal mean wind field reflect directly onto the waves, all eigenmodes of the system are coupled oscillations involving both nonzonal perturbations in the potential vorticity field and variations in the zonal mean velocity.

To apply the above equations to the initial value vacillation problem discussed in Lindzen et al. (1982), the following conditions need to be satisfied:

$$U_0^* + U_1^*(t = 0) = \overline{U}(t = 0), \tag{11a}$$

$$A_0^* + A_1^*(t = 0) = 0, \tag{11b}$$

$$B_1^*(t = 0) = 0. \tag{11c}$$

The general solutions can be given the form $U_1^*(t) = U_1^* \cos(\omega_1^* t)$, $A_1^*(t) = A_1^* \cos(\omega_1^* t)$, and $B_1^*(t) = B_1^* \sin(\omega_1^* t)$. The solution for the eddy field can thus be written as

$$\Psi_1^* = [A_1^* - (\pm B_1^*)] \cos(\omega_1^* t) \sin(kx) + (\pm B_1^*) \sin(kx \pm \omega_1^* t), \tag{12}$$

where the $\pm$ sign corresponds to subcritical and supercritical basic states, respectively. Using the initial condition of pure zonal symmetry (11b) one has

$$A_1^* = -A_0^*, \qquad B_1^* = \frac{\omega_1^*}{k\left(U_0^* - \frac{\beta}{k^2}\right)}A_0^*, \tag{13a}$$

$$U_1^*(t) = \frac{1}{2}\frac{\left(\frac{f_0}{H}h\right)^2}{k^2\left(U_0^* - \frac{\beta}{k^2}\right)^2}U_0^* \cos(\omega_1^* t). \tag{13b}$$

Imposing furthermore the condition (11a) on the initial zonal mean flow, we obtain

$$U_0^* + \frac{1}{2}\frac{\left(\frac{f_0}{H}h\right)^2}{k^2\left(U_0^* - \frac{\beta}{k^2}\right)^2}U_0^* = \overline{U}(t = 0). \tag{14}$$

Given $\overline{U}(t = 0)$ one can solve this third-order polynomial and find U_0^*, thus obtaining a full solution to the problem. A qualitative description of the flow evolution is, however, possible without explicitly solving for all variables. A simple inspection of the expressions above shows the separation of the eddy field into a steady amplitude traveling wave and an oscillating stationary wave, forced by vacillations in the zonal mean flow. It can be seen that the stationary wave decreases in amplitude as the traveling wave tends to get in phase with it and interfere positively, thus leading to a smaller maximum superposition amplitude than predicted by the linear solution of Lindzen et al. (1982).

A very important characteristic of the quasi-linear solution is that by construction it conserves both the total kinetic energy and potential enstrophy (Rambaldi and Flierl 1983; Charney and DeVore 1979), ensuring a nonlinear stability of the flow.[2] Thus, the quasi-linear solution suffers from no ''danger'' of excessive wave growth. The decrease of the stationary wave amplitude limits the maximum superposition amplitude and allows the flow to evolve without violating the potential enstrophy constraint.

While the results above were derived for a one-dimensional system, generalizing to a two-dimensional barotropic flow is relatively straightforward. Following Charney and DeVore (1979), one can represent the flow by a small number of spectral functions, obtaining a system of equations similar to the one presented above. One can then solve for the coefficients of the spectral

[2] The nonlinear stability is of course lost in the linearized version of the equations presented above. While the validity of our analytical solution is somewhat questionable, given that condition (11b) contradicts the small-amplitude assumption for Ψ_1^*, it is hoped that its main characteristics survive such simplifications.

functions representing the most basic structures in the flow. In simpler terms, one can modify the solutions presented above by substituting $k^2 + l^2$ for the total wavenumber square whenever appropriate.

5. Nonlinear flow—Parameter space

Given the above results, it is important to carefully span the parameter space of the fully nonlinear flow, and to examine the domain of validity of the simple quasi-linear solution as the topographic forcing increases to high values. As discussed in the previous section, the ability of the quasi-linear solution to limit wave amplitudes and prevent a violation of the potential enstrophy constraint comes as a result of the modification of the stationary wave amplitude by the decelerated zonal mean flow. Also, as mentioned in section 3, the formation of zonal mean easterly winds ultimately appears to be crucial for the wave saturation. To the degree that this is true one expects the nonlinear flow to deviate most strongly from a wave–mean flow interaction pattern in situations where the wave drag is least efficient in decelerating the zonal mean flow. Thus, to check for limitations of the quasi-linear solution, one should look for configurations that allow large wave growth while keeping the zonal mean flow relatively unchanged.

In the linear solution of Lindzen et al. (1982), the variations of the zonal mean flow were given by

$$\delta U = -A_1\left(\frac{1}{4}\frac{f_0}{H}h\frac{1}{c}\right)[1 - \cos(2ly)][1 - \cos(kct)], \quad (15)$$

where A_1 is the amplitude of the stationary wave, or half the amplitude of the maximum wave superposition. Using the relation $A_1 = (U_0/c)[1/(k^2 + l^2)][(f_0/H\,h)]$ one can rewrite the expression above in terms of A_1 and the basic-state wind U_0:

$$\delta U = -\frac{1}{4}(k^2 + l^2)\frac{A_1^2}{U_0}[1 - \cos(2ly)] \times [1 - \cos(kct)]. \quad (16)$$

At the time of maximum modification of the zonal mean flow the deviation of the mean velocity, in the center of the channel, from the basic-state velocity U_0 can be shown to be

$$|\delta U|_{\max} = (k^2 + l^2)\frac{A_1^2}{U_0}. \quad (17)$$

Therefore, the minimum value for the zonal mean velocity, in the center of the channel, will be given by

$$U_{\min} = U_0 - |\delta U|_{\max} = U_0 - (k^2 + l^2)\frac{A_1^2}{U_0}. \quad (18)$$

The expression above shows that for a given wave amplitude A_1 the reduction of the zonal mean winds is smaller as the basic-state velocity U_0 becomes more strongly westerly. In other words, for strong westerly basic states one can reach high wave amplitudes before the deceleration by the wave drag manages to produce easterly mean winds. To the degree that the growth of the waves leads toward a violation of the potential enstrophy constraint it suggests the possibility of a breakdown of the quasi-linear solution for strongly westerly basic states, and a stronger deviation from the wave–mean flow type of interactions.

6. Numerical runs—Model setup

To investigate the behavior of the fully nonlinear flow a quasigeostrophic, barotropic beta-plane channel numerical model is used. The model is forced with a topography of zonal wavenumber one and a meridional half-wavelength equal to the total width of the domain. As an initial condition a zonal mean flow of strength U_0 is imposed. The dimensions of the numerical domain are taken as $L_x = 30\,000$ km and $L_y = 5000$ km. Thus, the waves forced by the topography have dimensions characteristic of stratospheric planetary waves. Also, the planetary vorticity and planetary vorticity gradient take values characteristic of midlatitude regions, $f_0 = 1.0 \times 10^{-4}$ s^{-1} and $\beta = 1.6 \times 10^{-11}$ m^{-1} s^{-1}. The depth of the fluid is arbitrarily chosen $H = 10\,000$ m.

Given the above values for the various variables, the westward phase speed, relative to the mean flow, for waves of the scale of the topography is $\beta/(k^2 + l^2) = -36.5$ m s^{-1}. In order to fully span the parameter space of the model basic state, velocities U_0 with values of 10, 18, 33, and 46 m s^{-1} have been used, the first three choices corresponding to subcritical basic states ($U_0 - \beta/(k^2 + l^2) < 0$), with the fourth one being supercritical ($U_0 - \beta/(k^2 + l^2) > 0$). While in a three-dimensional atmosphere supercritical mean flows lead to vertical trapping and evanescence of the forced stationary disturbance, in a barotropic model the differences between subcritical and supercritical flows are not as evident. The sign of the stationary wave vorticity anomalies over the topographic troughs and ridges reverses as the mean flow turns supercritical, but no other consequence is immediately apparent.

The horizontal grid spacing in the numerical model is taken $dx \simeq 500$ km and $dy = 100$ km, corresponding to 64 grid points in the zonal direction and 50 grid points in the meridional. To conserve kinetic energy, potential energy, and potential enstrophy, the Arakawa formulation for the calculation of the Jacobian is used, and a simple leapfrog scheme is used for the forward time integration. Finally, a del-sixth diffusion operator, acting on the streamfunction field, is used to dissipate small-scale disturbances, but no further damping is applied to the flow. The diffusion coefficient is chosen $A_h = 4.0\ 10^{15}$ m^4 s^{-1}, corresponding to time scales of 1/4 day and 10 000 days for the smallest and largest scales, respectively. As numerical runs with a diffusion coefficient reduced by a factor of 10 show no appreciable change in the evolution of the flow, despite the signif-

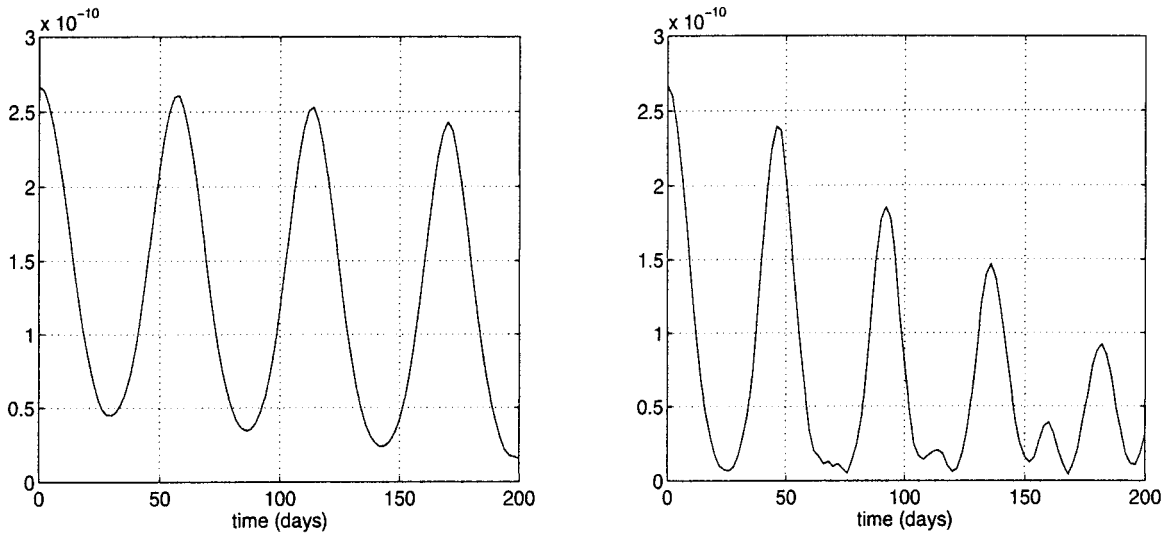

FIG. 1. Time evolution of the mean available potential enstrophy. (Units: s^{-2}). Basic state $U_0 = 33$ m s^{-1}. Left: $h = 400$ m. Right: $h = 600$ m.

icantly stronger presence of small scales in the potential vorticity maps, it is concluded that our results are not sensitive to changes in the effective resolution of the model.

7. Numerical results

For each basic state a series of numerical runs is conducted, each model integration corresponding to a different height of the bottom topography, covering a range of values such as to go well beyond the point at which the linear solution of Lindzen et al. (1982) is expected to break down. In each case the evolution of the flow is followed through the first few vacillation cycles.

Interestingly, the time evolution of the nonlinear flow is dominated by quasiperiodic vacillations even at high forcing amplitudes (see Fig. 1). Naturally, as the topographic forcing increases, the deformation of the flow becomes stronger and the time evolution of the flow does not retain a nice periodic character for more than a few vacillation cycles. The decay of the observed oscillations is not, however, a result of strong energy or potential enstrophy dissipation, as the flow is found to evolve in a mostly conservative fashion even for the strongest forcing values. For the results corresponding

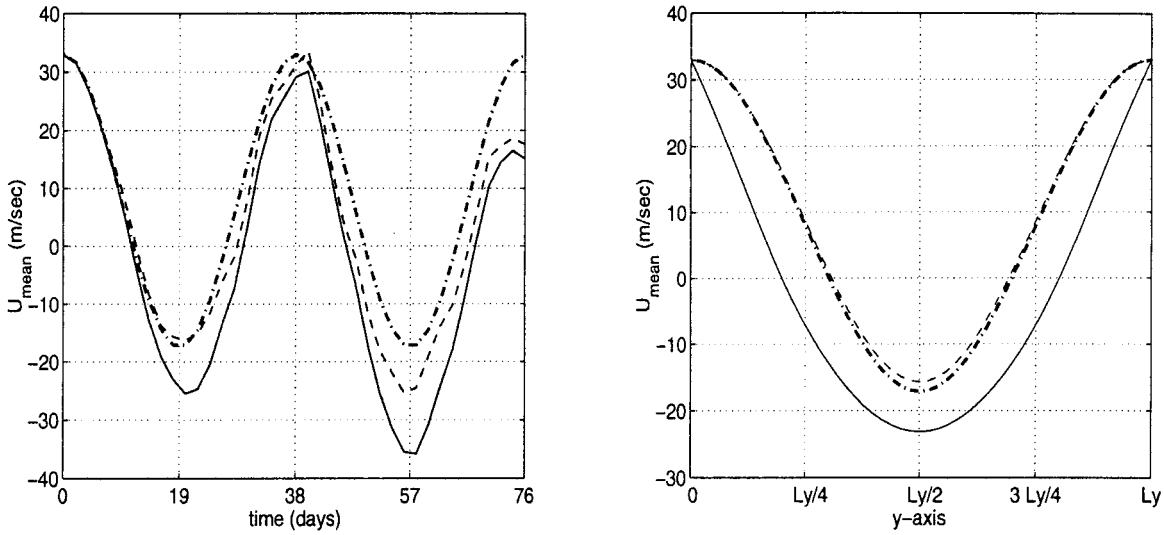

FIG. 2. True zonal mean velocity field (solid line) and reconstruction obtained by retaining only $\tilde{U}_1$ (thin dashed line) and $\hat{U}_{1,1}$ (thick dash–dot line). $U_0 = 33$ m s^{-1}, $h = 800$ m. Left: Time series of velocity values at the center of the channel. Right: Meridional profile at time of maximum wave growth.

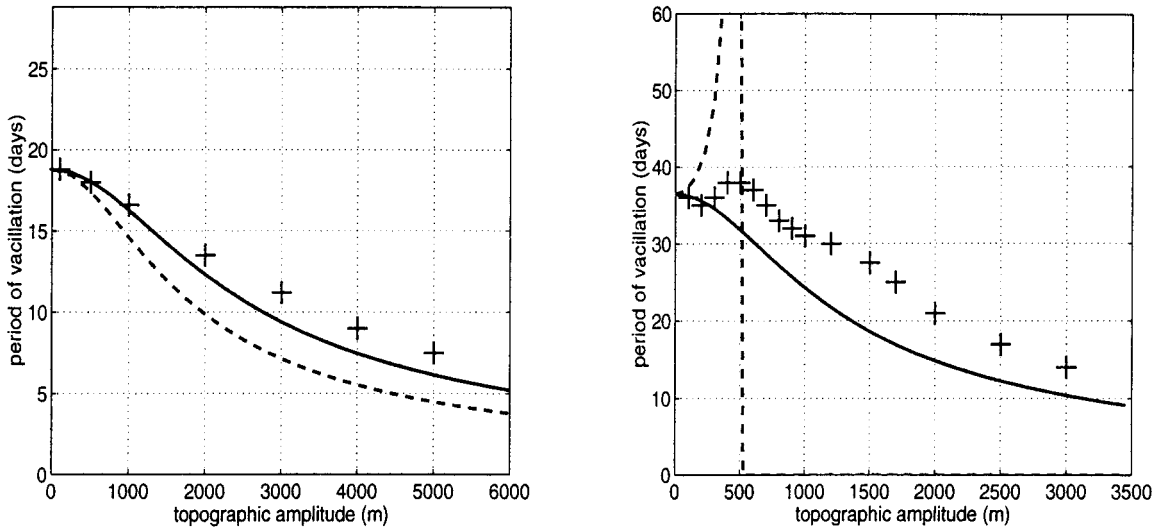

FIG. 3. Comparison between the period of vacillation obtained in the numerical model (+) and the prediction of the quasi-linear analytical solution for $A_0^* = 0$ (solid line) and $A_0^* = A_{\text{linear}}$ (dashed line), respectively. Left: $U_0 = 18$ m s^{-1}. Right: $U_0 = 46$ m s^{-1}.

to Fig. 1, with $h = 600$ m, the loss of energy and potential enstrophy over the total 200-day period is only about 10% and 30%, respectively. Thus the deviations from the perfectly periodic vacillation cycles at large times seem to be due to shearing of the large-scale waves and to the continuous cascade of enstrophy and energy to smaller scales that results from wave–wave interactions. Still, the overall persistence of the periodic behavior, even at forcing values that are well outside the validity range of linear theory, is quite striking.

To compare the nonlinear flow evolution with the predictions of the quasi-linear analytical solution the results of each numerical run are analyzed for the first two vacillation cycles. While an analysis of the zonal mean flow is straightforward, the same is not true for the eddy field; no direct method exists for separating the wave-1 field into a traveling and a stationary component, given that the amplitudes of both components could be time varying. Using, however, the linear solution of Lindzen et al. (1982) an indirect estimation of the traveling wave amplitude is possible.

Assuming a steadily propagating wave, of constant amplitude $\|\Psi_{tr}\|$, and wavenumber (k, l), the linear solution of Lindzen et al. (1982) [see Eq. (3c)] predicts a time variation of the zonal mean winds such that

$$\delta U = -\frac{1}{4}\left(\frac{f_0}{H}h\right)\frac{1}{c}\|\Psi_{\text{tr}}\|[1 - \cos(2ly)] \times [1 - \cos(kct)]. \quad (19)$$

This formula allows one to use the observed variations in the zonal mean flow and invert for the amplitude of the traveling wave. Decomposing the zonal mean velocity in terms of cosine basis functions in space and time, one has

$$U(y, t) = \sum_{n=0}^{N} \tilde{U}_n(t) \cos\left(n\frac{2\pi}{L_y}y\right) = \sum_{n=0}^{N}\sum_{m=0}^{M} \hat{U}_{n,m} \cos\left(n\frac{2\pi}{L_y}y\right)\cos\left(m\frac{2\pi}{T}t\right). \quad (20)$$

Retaining only the gravest modes from the cosine expansion in y and t, one can approximately reconstruct the variations in the zonal mean velocity field as

$$\tilde{U} = U_0 + \tilde{U}_1(t)\left[1 - \cos\left(\frac{2\pi}{L_y}y\right)\right] \quad (21)$$

$$\hat{U} = U_0 + \hat{U}_{1,1}\left[1 - \cos\left(\frac{2\pi}{L_y}y\right)\right]\left[1 - \cos\left(\frac{2\pi}{T}t\right)\right]. \quad (22)$$

To the degree that variations of the zonal mean flow are indeed well captured by the representation above one can invert for the traveling wave amplitude, using Eq. (19),

$$\|\Psi_{\text{tr}}\| = -\frac{1}{\frac{1}{4}\left(\frac{f_0}{H}h\right)\frac{1}{c}}\hat{U}_{1,1}, \qquad c = \omega k = \frac{2\pi}{T_{\text{observed}}}k, \quad (23)$$

where T_{observed} is the dominant period observed in the mean flow vacillations. Naturally the accuracy of the above estimate of $\|\Psi_{\text{tr}}\|$ depends on how well the time varying zonal mean flow in the nonlinear model can be represented by the expression $U_0 + \hat{U}_{1,1}(1 - \cos((2\pi/L_y)\, y))(1 - \cos((2\pi/T)\, t))$. Generally the above approximation is found to be reasonably good, even for high topographic forcing values, when the deformation of the flow becomes large (see Fig. 2). Given this good agreement one can use the results obtained for the trav-

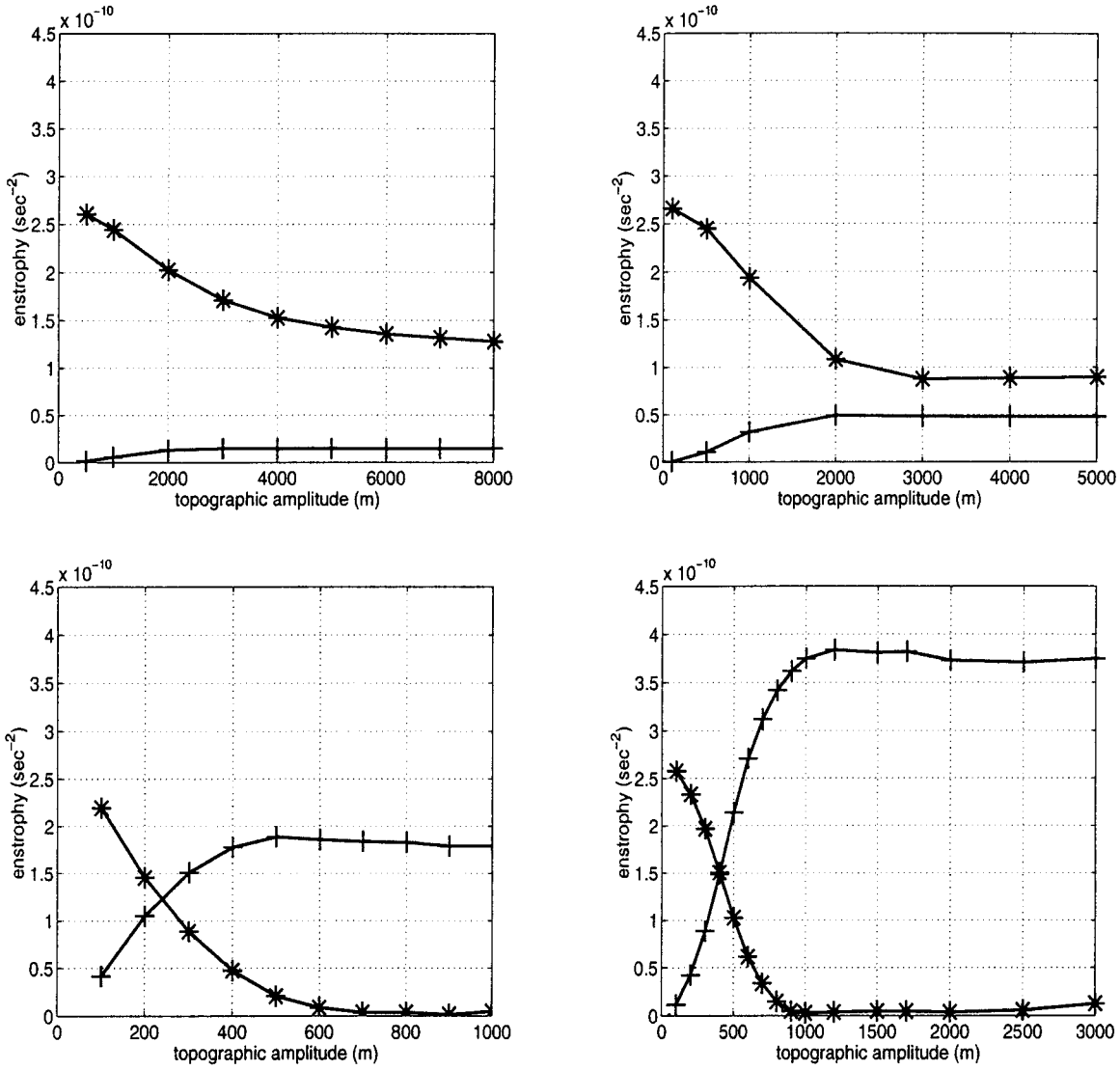

FIG. 4. Evolution of maximum wavenumber (k, l) enstrophy (+) and minimum mean available potential enstrophy (*), as functions of the topographic forcing. Results for four different basic states: $U_0 = 10$, 18, 33, and 46 m s^{-1}, going from left to right and from top to bottom.

eling wave amplitude with relative confidence. Moreover, the fact that the quasi-linear solution predicted a steady amplitude traveling wave adds to the credibility of the above calculations.

Given an estimate of the traveling component one can proceed in estimating the stationary wave amplitude as well, subtracting Ψ_{tr} from the total wavenumber (k, l) eddy field. The time evolution of the estimated stationary wave amplitude is found to agree well with the quasi-linear prediction, showing a vacillation with time, in response to the variations of the zonal mean flow. The stationary wave is seen to decrease in amplitude as the mean flow is decelerated, thus helping in reducing the maximum wave superposition amplitude with respect to the prediction of the linear solution.

The above results suggest a good correspondence between the nonlinear model results and the quasi-linear prediction. However, the most striking characteristic of the nonlinear flow is perhaps the increase in the vacillation frequency as the topographic forcing increases (see Fig. 3). While the modification of the zonal mean velocity and potential vorticity gradient is strong, calculations of eigenmodes propagating on the instantaneous mean flow show no significant changes in the phase speed of free Rossby waves. Thus the observed changes in the period of vacillation cannot be accounted for by changes in the zonal mean flow. On the other hand, the quasi-linear solution does predict a dependence of the vacillation eigenfrequency on the topographic amplitude:

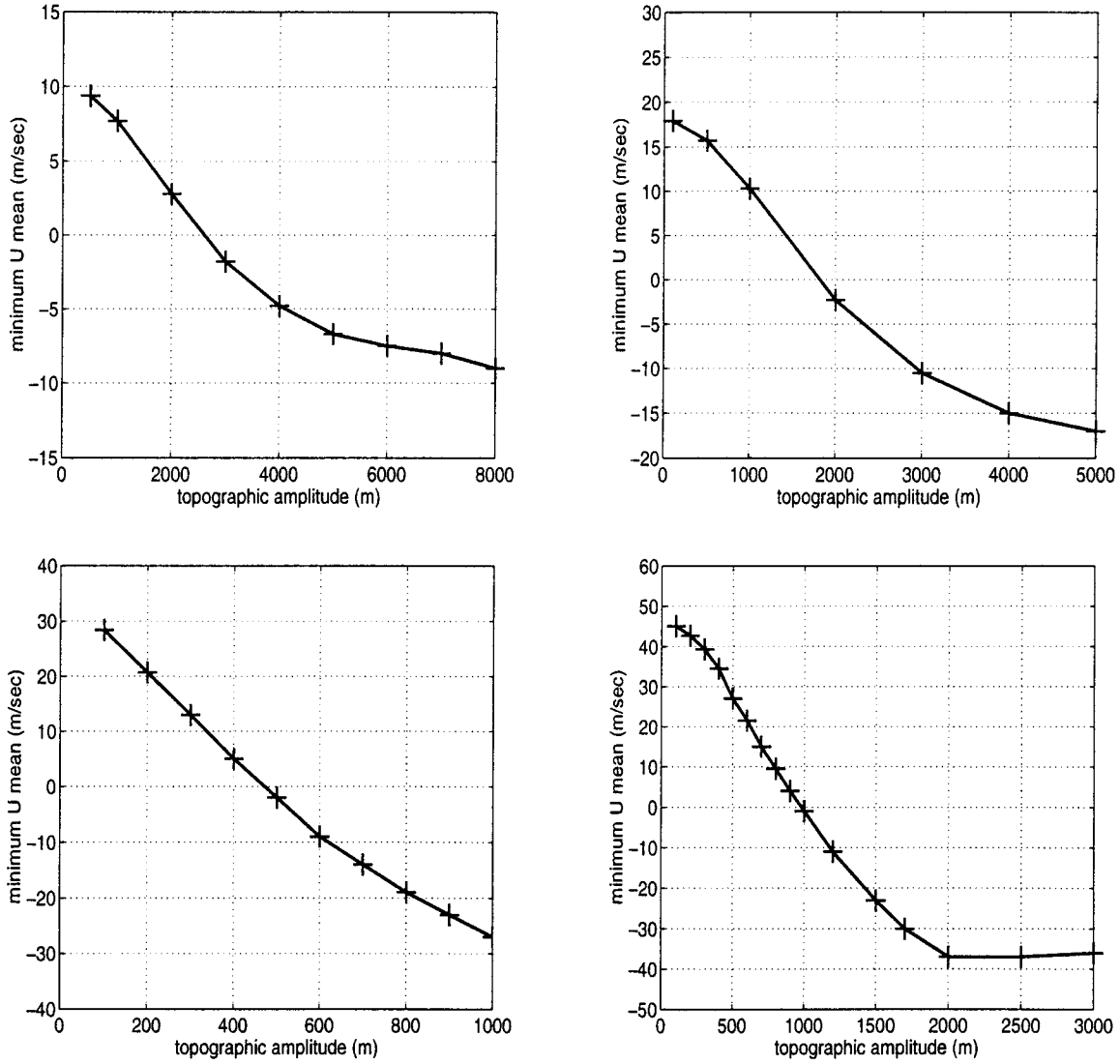

FIG. 5. Minimum zonal mean wind, averaged over the center of the channel, as a function of the topographic forcing. Results for four different basic states: $U_0 = 10$, 18, 33, and 46 m s^{-1}, going from left to right and from top to bottom.

$$\omega_1^* = \sqrt{\left(U_0^* - \frac{\beta}{k^2}\right)^2 k^2 + \frac{1}{2}\left(\frac{f_0}{H}h\right)\left(-A_0^* + \frac{1}{k^2}\frac{f_0}{H}h\right)k^2}. \tag{24}$$

To apply the above formula one needs to estimate the value of U_0^* corresponding to each topographic amplitude. As U_0^* represents the time mean zonal mean velocity one could directly refer to the model output. Alternatively, one can use Eq. (14), given h and $\overline{U}(t = 0) = U_0$. Choosing the appropriate root for U_0^* one can calculate A_0^* and proceed in evaluating ω_1^*.

One slight complication arises from the fact that the expression above only includes information about the time mean zonal flow through the estimate of U_0^* and fails to use an appropriate effective β. In other words, it fails to estimate correctly the phase speed c of *free* Rossby waves propagating through the time mean zonal flow. As mentioned above, one seems to have a relative invariance of c for modes with scales similar to that of the topography. In other words, despite the strong changes in the mean velocity and potential vorticity gradient, the phase speed of *free* waves does not seem to be strongly affected. Thus one would be justified, to some degree, in substituting $(U_0 - \beta/k^2)$ for $(U_0^* - \beta/k^2)$ in expression (24).

A second point, however, concerns the appearance of A_0^*, the time mean stationary wave, in the expression for ω_1^*. In the one-dimensional formulation of Rambaldi and Flierl (1983), oscillations of the zonal mean winds U_{1*} lead to forcing of transient eddy components partly due to the term $U_1^*(\partial/\partial x)(\partial^2\Psi_0^*/\partial x^2)$ that appears in Eq. (8b). Physically this can be viewed as the forcing of transients due to the wobbling of the position of the

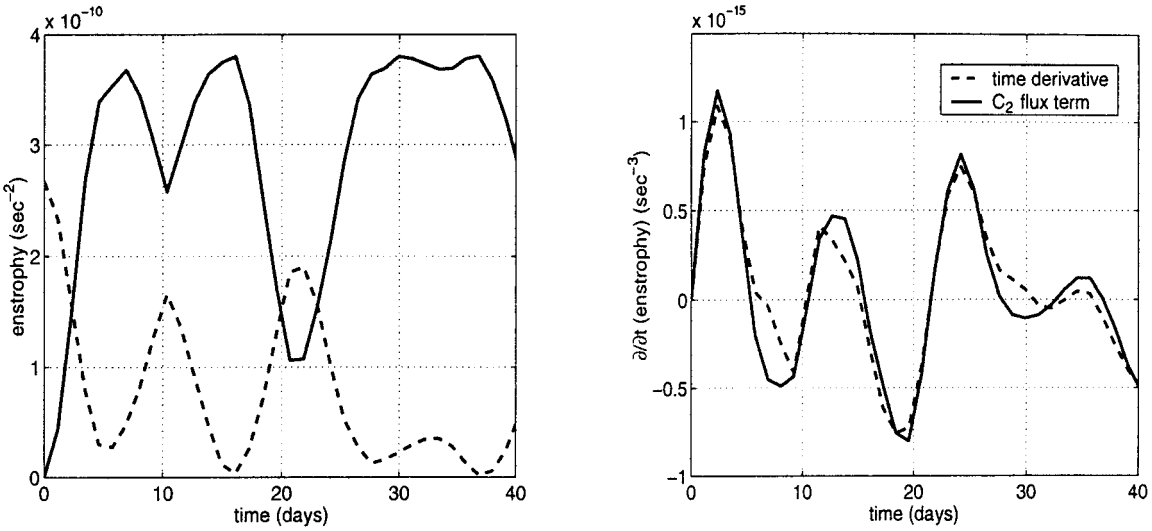

FIG. 6. Left: Time series of wavenumber (k, l) enstrophy (solid line) and mean available potential enstrophy (dashed line) for $U_0 = 46$ m s^{-1} and $h = 2000$ m. Right: Comparison between time tendency of wavenumber (k, l) enstrophy and term C_2.

stationary wave. The one-dimensional system, however, fails to take into account the meridional advection of the relative vorticity associated with the oscillating zonal mean flow by the time mean stationary wave. Because in Rambaldi and Flierl (1983) the zonal mean flow is homogeneous in y, variations in U^* do not affect the mean meridional potential vorticity gradient.

For a two-dimensional system, however, one should add a term, $\partial\Psi_0^*/\partial x(-\partial^2 U_1^*/\partial y^2)$. Interestingly, this term tends to counterbalance the effect of $U_1^*(\partial/\partial x)(\partial^2\Psi_0^*/\partial x^2)$. While a weakening (strengthening) of the zonal mean winds U^* tends to advect the potential vorticity of the time mean stationary wave westward (eastward), the corresponding modification of the zonal mean potential vorticity gradients has the opposite effect. The degree to which these two terms counterbalance each other is not clear a priori, of course. Given, however, the relative invariance of the phase speed c of *free* waves that was found, it appears that one has a near-perfect cancellation. Such cancellation between the effects of changes in the mean flow and changes in potential vorticity gradient was also noted by Simmons (1974).

A straightforward way to address this problem is by comparing the model results with the analytical predictions one obtains under two extreme assumptions; in one case one completely neglects the term representing the time mean stationary wave, setting $A_0^* = 0$, while in the other case one uses the formula for the one-dimensional solution without any further modifications, setting $A_0^* = A_{\text{linear}} = U_0/c[1/k^2 + l^2](f_0/H\,h)$. The comparison of the results obtained in each case with the behavior observed in the numerical model is shown in Fig. 3. One sees that the calculations corresponding to $A_0^* = 0$ give much better agreement with the numerical model results, particularly in the case of $U_0 = 46$ m s^{-1}, while including a term $A_0^* = A_{\text{linear}}$ leads to a complete breakdown of the calculations. Of course, rather than arbitrarily setting $A_0^* = 0$ based solely on the qualitative arguments presented above, one can proceed to a more rigorous calculation by reformulating the quasi-linear solution so as to include information about the meridional structure of the flow. Expressing the eddy components in terms of $\sin(ly)$ functions and the zonal mean velocity as $U^* = U_0^* + U_1^*[1 - \cos(2ly)]$ one gets an expression for the eigenfrequency of vacillations that is

$$\omega_1^* = \sqrt{\left(U_0^* - \frac{\beta}{k^2 - l^2}\right)^2 k^2 + \frac{1}{4}\left(\frac{f_0}{H}h\right)\left[-\left(\frac{3}{2} - \frac{1}{2}\frac{4l^2}{k^2 - l^2}\right)A_0^* + \frac{3}{2}\frac{1}{k^2 - l^2}\frac{f_0}{H}h\right]k^2}. \tag{25}$$

While uncertainty about the various numerical factors can lead to differences in the final results, the overall behavior appears to follow reasonably well the prediction obtained with the simple formula and the choice of $A_0^* = 0$. Thus our interpretation, that changes in the zonal mean velocity and in the zonal mean potential vorticity gradient tend to counteract each other, appears to be correct and the quasi-linear solution proves ca-

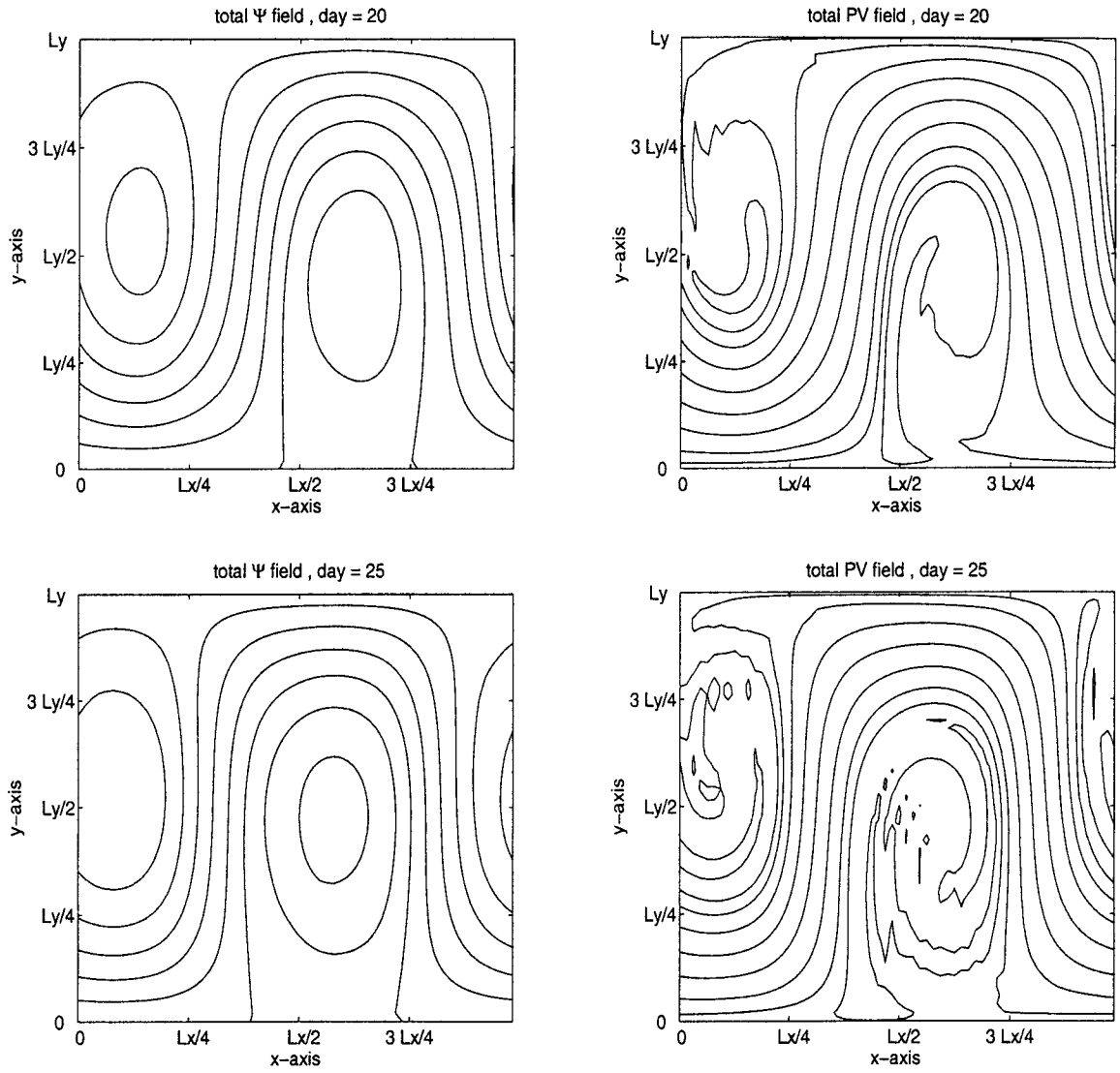

FIG. 7. Snapshots of the streamfunction and potential vorticity evolution for the case $U_0 = 33$ m s^{-1} and $h = 400$ m.

pable of predicting the behavior of the numerical model with surprising success. This is particularly impressive in view of the simplifications involved in the analytical calculations.

All of the above results show a persistence of the quasi-linear solution even at high topographic forcing values. Given the original anticipation that the potential enstrophy constraint might force deviations from a wave–mean flow interaction pattern it is interesting to examine the flow evolution from a potential enstrophy perspective. Analyzing the model results in terms of the maximum attained enstrophy of the (k, l) wave and the minimum mean available potential enstrophy, where minima and maxima refer to the values of the respective quantities over the first vacillation cycle, one observes a saturation of the wave enstrophy at strong topographic forcing values (see Fig. 4). While this is hardly unexpected, given the limit placed on wave amplitudes by the potential enstrophy constraint, the interpretation of the dynamics leading to wave saturation is not straightforward.

The first point to note is that saturation of the wave growth is found to occur at different levels of eddy enstrophy for each basic state. As the eddy potential enstrophy is $\overline{(1/2)(\zeta' + (f_0/H)\, h)^2}$, the saturation value for the eddy enstrophy, $\overline{(1/2)\zeta'^2}$, is not necessarily particularly revealing on its own (for a discussion of how the potential enstrophy and other constraints can be used to estimate a bound on wave growth, see the appendix). What is interesting, however, is that the wave saturation does not seem to come as a result of depletion of the mean available potential enstrophy. This is particularly obvious for weakly westerly basic states (see Fig. 4), where saturation of the waves occurs despite the large amount of available potential enstrophy retained in the modified mean flow.

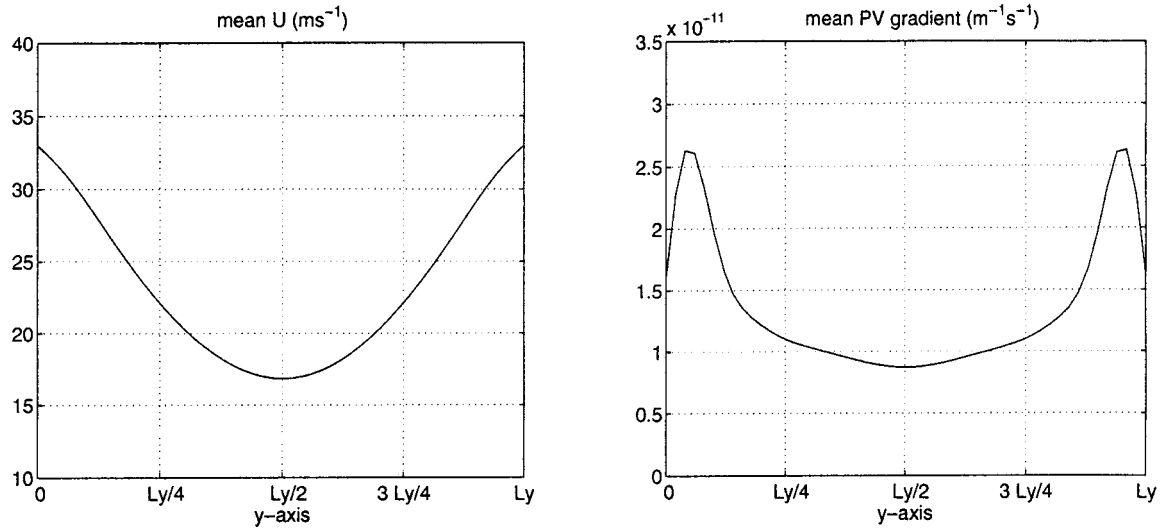

FIG. 8. Meridional profile of the deformed zonal mean flow on day 12. Basic state $U_0 = 33$ m s^{-1}, $h = 500$ m. Left: Zonal mean velocity. Right: Zonal mean potential vorticity gradient.

In section 3 it was argued that the formation of zonal mean easterly winds might lead to saturation of wave growth. As the results of Fig. 4 suggest that the wave saturation process is not related to the potential enstrophy constraint, it is important to check the possibility that the deceleration of the mean winds might indeed play a role in limiting the wave amplitudes. Comparing the maximum wavenumber (k, l) enstrophy values obtained from the various numerical runs with the respective minimum values for the zonal mean winds, where minimum refers to wind variations over the first vacillation cycle and where the winds are averaged over the central half of the channel so as to be representative of a large fraction of the domain, it is observed that the wave enstrophy saturation largely coincides with the first appearance of zonal mean easterlies (see Fig. 5). As can be seen, the value of h at which mean easterlies first form does indeed coincide with the topographic amplitude for which the wave enstrophy reaches its saturation limit.

While the simple graphic comparison does not constitute a quantitatively convincing argument, it is certainly strongly suggestive of a connection between the formation of mean easterlies and the saturation of the wave amplitudes. However, to examine quantitatively the dynamics leading to the wave saturation one needs to resort to an analysis of the enstrophy budget for the wavenumber (k, l) disturbance. As shown in section 3, it is indeed possible to separate between the various terms affecting the evolution of the eddy enstrophy and to distinguish between the different physical processes involved. Thus one can examine the contribution of wave–mean flow interactions, versus wave–wave interactions and higher nonlinearities in the enstrophy budget, and how their relative importance changes as the topographic forcing increases:

$$\frac{\partial}{\partial t}\frac{\langle\overline{\zeta'^2_{k,l}}\rangle}{2} = \underbrace{\left\langle\overline{\zeta'_{k,l}\left[-\frac{\partial\Psi'_{k,l}}{\partial x}\left(\beta + \frac{\partial\overline{\zeta}}{\partial y}\right)\right]}\right\rangle}_{C_1} + \underbrace{\left\langle\overline{\zeta'_{k,l}\left[-\overline{u}\frac{f_0}{H}\frac{\partial h'}{\partial x}\right]}\right\rangle}_{C_2} + \underbrace{\left\langle\overline{\zeta'_{k,l}\left[-\sum_N\sum_M J\left(\Psi'_{N,M}, \frac{f_0}{H}h'\right)\right]}\right\rangle}_{C_3}. \tag{26}$$

Term C_2 reflects the effect of changes in the topographic forcing and is straightforward to calculate. Comparing its time evolution with the time tendency of the wavenumber (k, l) enstrophy one can specify the degree to which changes in the mean winds are indeed responsible for limiting the wave growth. Such a comparison, for the case of $U_0 = 46$ m s^{-1} and $h = 2000$ m, is shown in Fig. 6. As shown, the time variations of term C_2 coincide quite well with the observed wave enstrophy time tendency. The other terms in the enstrophy budget seem to be of minor importance, despite the high amplitude of the topographic forcing and the strong deformation of the flow that is observed at this value of the topographic forcing.

A careful inspection of the time evolution of C_2 and of the time evolution of the zonal mean winds clearly shows how the formation of zonal mean easterlies coincides with a reversal in the tendency of the wave enstrophy to grow, starting from day 7 of the numerical integration. The identification of the zonal wind reversal as the controlling mechanism in the saturation of the forced wave in the nonlinear flow also explains the differences in the level at which the wave enstrophy saturates for different basic states (see Fig. 4). Indeed, as argued in section 5, for weaker westerly basic states the wave drag term produces easterlies more easily than in the case of strongly westerly U_0. Thus the level of wave saturation is higher for the more strongly westerly basic states, $U_0 = 33$ m s^{-1} and $U_0 = 46$ m s^{-1}.

8. Discussion and summary

The barotropic model is a convenient tool for addressing the issue of wave saturation and the relevance of the potential enstrophy constraint in the saturation process. The simplicity of the model allows for a relatively clear examination of the nonlinear flow dynamics, at a small numerical cost, even at the high resolution necessary to capture the full range of dynamical interactions. Perhaps the most surprising finding of the present study is that the potential enstrophy constraint proves to be largely irrelevant to the flow dynamics. For weakly westerly basic states the saturation of wave growth comes without any sign of depletion of the mean available potential enstrophy. Even in the cases of strongly westerly basic states, where the zonal mean flow is modified to the point where the mean available potential enstrophy is completely depleted, the mechanism ultimately found to be responsible for the wave saturation proves not to be directly related to this depletion.

On the whole, wave–wave interactions are found to be of secondary importance to the evolution of the flow, contrary to the general perception of how nonlinear Rossby wave saturation occurs (Garcia 1991; McIntyre and Palmer 1985). This is not to say, of course, that wave–wave interactions are nonexistent. Figure 7 shows clearly the signature of such interactions, as manifested in the potential vorticity field. The deformation of the potential vorticity field by nonlinear advection has the familiar signature of Rossby wave breaking, with stretching and wrapping of the potential vorticity contours in the regions of closed circulation. However, the analysis of the numerical results shows that the most important aspects of the dynamics of the flow can be understood by focusing purely on the interaction between the forced wave and the zonal mean flow. As it turns out, quasi-linear interactions are sufficient in constraining the wave growth and leave no room for wave–wave interactions to become important, even for the strongest topographic forcings.

These results are intriguing for the implications they might have for the case of vertically propagating waves and for our understanding of stratospheric dynamics. However, before attempting such a connection a few further comments are necessary. As our conclusions, concerning the importance of wave–wave interactions, appear to contrast other studies that highlight wave breaking as being of first-order importance in the dynamics (Juckes and McIntyre 1987; Polvani et al. 1995), a closer look at our model setup is necessary. It can certainly be argued that our model configuration, with the topography having a meridional half-wavelength equal to the total width of the domain, constrains to some degree the dynamics of the flow. As a downscale enstrophy cascade necessitates a simultaneous upscale cascade of energy, our configuration could artificially suppress wave–wave interactions. In more simple terms, a model setup where the topography is confined latitudinally to only a certain part of the domain would leave more freedom to the forced wave to propagate meridionally and might allow for a stronger role of wave–wave interactions in the wave saturation.

Numerical runs, however, with meridionally expanded domains and a topography that either maintains a perfectly sinusoidal shape in the meridional, with more wavelengths contained in the domain, or is confined to the central part of the domain only do not show significant qualitative differences. That might of course not be the case if one were interested in a final equilibrated state. However, for the vacillation problem, the evolution of the flow during the first cycle seems in all cases to be reasonably described in terms of the behavior observed in the simple model. To properly address the issue of the long time limit and of the dynamical balance that characterizes the equilibrated flow, one would need to use some restoring mechanism for the zonal mean flow, such as used in Polvani et al. (1995). It is worth noting, however, that while in that study wave breaking clearly plays an important role in affecting the mean flow structure in the final state, it is not obvious how strong the direct effect of wave–wave interactions on the forced wave is.

In any case, a direct translation of our results to the vertical propagation case is not straightforward. For one thing there is no direct counterpart in the three-dimensional case of the saturation mechanism obtained in the barotropic model, where the saturation dynamics rely on the deceleration of the mean flow to easterlies. However, the modification of the zonal mean flow observed in the barotropic model does offer some hints about the possible patterns of interaction in the three-dimensional model. For example, the deformation of the zonal mean wind field is seen to lead to a decrease in the zonal mean potential vorticity gradient in the center of the channel (see Fig. 8). Such a reduction, in the three-dimensional case, could lead to negative index of refraction square values and a reduction of the ability of the forced wave to propagate in the vertical, thus leading to saturation. The fact that the barotropic model is capable of limiting

wave growth through a purely quasi-linear mechanism and that wave–wave interactions never become significant suggests that a similiar picture might arise in the three-dimensional case as well.

Of course it is not possible to extend much further the conclusions drawn from the barotropic model. A proper discussion of the vertical propagation problem would require a careful numerical investigation with a three-dimensional model. Thus far, while a small number of three-dimensional numerical studies, examining the nonlinear flow response to strong vertical penetration of a forced wave, do exist (O'Neill and Pope 1988; Robinson 1988; Dritschel and Saravanan 1994), none of them has explicitly approached the issue of wave saturation. We are currently undertaking such a study, focusing again on relatively simple flow configurations, and results will be presented in forthcoming papers.

Acknowledgments. The authors would like to thank Glenn Flierl and Alan Plumb for many useful discussions and suggestions. The suggestions of the anonymous reviewers were very helpful as well. Support for this research came from Grants ATM-9813795 from the National Science Foundation, NAG5-6304 from the National Aeronautics and Space Administration, and DEFG02-93ER61673 of the Department of Energy (DOE-CCPP).

APPENDIX

Simple Upper Bounds

A simple upper bound on eddy amplitudes can be derived from the potential enstrophy constraint; the maximum eddy potential enstrophy cannot exceed the initial mean available potential enstrophy. Taking as a starting point conservation of potential vorticity one gets

$$\frac{1}{A}\int \frac{1}{2}\left[q(t) - \frac{1}{A}\int \beta y\, dA\right]^2 dA = \frac{1}{A}\int \frac{1}{2}\left[q(0) - \frac{1}{A}\int \beta y\, dA\right]^2 dA. \quad \text{(A1)}$$

Here A is the horizontal area of the domain and $q = \nabla^2\Psi + \beta y + (f_0/H)\, h'$. Separating into a zonal mean component (overbars) and eddies (primes), one has

$$\frac{1}{L_y}\int_0^{L_y} \frac{1}{2}\overline{\left[\nabla^2\Psi'(t) + \frac{f_0}{H}h'\right]^2}\, dy - \frac{1}{L_y}\int_0^{L_y} \frac{1}{2}\left(\overline{\frac{f_0}{H}h'}\right)^2 dy \le \frac{1}{24}\beta^2 L_y^2. \quad \text{(A2)}$$

Constraining the eddy potential enstrophy is straightforward. The same is not true, however, for the eddy enstrophy $\overline{1/2(\nabla^2\Psi')^2}$, due to uncertainties about the phasing between $\nabla^2\Psi'$ and h' at the time of maximum eddy growth. Moreover, while indeed representing an absolute upper bound, the potential enstrophy constraint alone significantly overestimates in some cases the eddy saturation amplitudes obtained in the numerical model. For more realistic estimates of the maximum amplitudes the growing eddies are expected to reach, additional information about the initial energy of the flow needs to be considered.

Use of such additional constraints is possible for the quasi-linear system of equations of Rambaldi and Flierl (1983), as two independent conserved quantities, E_0 and Q_0, can be shown to exist:

$$E_0 = U^{*2} + \frac{1}{2}k^2(A^{*2} + B^{*2}), \quad \text{(A3)}$$

$$Q_0 = \left(U^* - \frac{\beta}{k^2}\right)^2 + \frac{f_0}{H}hA^*. \quad \text{(A4)}$$

Here E_0 represents the total kinetic energy, while Q_0 represents a combination of kinetic energy and potential enstrophy. Given initial conditions one can solve this pair of equations and maximize the eddy enstrophy $(k^4/2)(A^{*2} + B^{*2})$. One is searching for the minimum possible U^*, given h and values for E_0 and Q_0, under the constraint that solutions for A^* and B^* remain real. Carrying the calculation to high values of h we obtain an estimate for the saturation eddy enstrophy. Results from

TABLE A1. Comparison between numerical results and estimates based on the quasi-linear system of equations for the maximum eddy enstrophy. Units for eddy enstrophy in s^{-2}.

h (m)	$\langle \overline{1/2 q_1^2} \rangle_{num}$	$\langle \overline{1/2 q_1^2} \rangle_{anal}$	h (m)	$\langle \overline{1/2 q_1^2} \rangle_{num}$	$\langle \overline{1/2 q_1^2} \rangle_{anal}$
	$U_0 = 10$ m s^{-1}			$U_0 = 18$ m s^{-1}	
500	$1.67\ 10^{-12}$	$2.85\ 10^{-12}$	500	$1.06\ 10^{-11}$	$1.49\ 10^{-11}$
1000	$5.70\ 10^{-12}$	$7.52\ 10^{-12}$	1000	$3.20\ 10^{-11}$	$2.93\ 10^{-11}$
2000	$1.31\ 10^{-11}$	$1.09\ 10^{-11}$	2000	$4.94\ 10^{-11}$	$3.55\ 10^{-11}$
3000	$1.47\ 10^{-11}$	$1.09\ 10^{-11}$	3000	$4.71\ 10^{-11}$	$3.55\ 10^{-11}$
4000	$1.47\ 10^{-11}$	$1.09\ 10^{-11}$	4000	$4.45\ 10^{-11}$	$3.55\ 10^{-11}$
	$U_0 = 33$ ms^{-1}			$U_0 = 46$ ms^{-1}	
100	$4.28\ 10^{-11}$	$2.97\ 10^{-11}$	200	$4.24\ 10^{-11}$	$1.97\ 10^{-10}$
200	$1.08\ 10^{-10}$	$5.46\ 10^{-11}$	400	$1.48\ 10^{-10}$	$2.18\ 10^{-10}$
300	$1.53\ 10^{-10}$	$7.19\ 10^{-11}$	600	$2.70\ 10^{-10}$	$2.27\ 10^{-10}$
600	$1.89\ 10^{-10}$	$1.02\ 10^{-10}$	1000	$3.76\ 10^{-10}$	$2.32\ 10^{-10}$
800	$1.85\ 10^{-10}$	$1.07\ 10^{-10}$	2000	$3.73\ 10^{-10}$	$2.32\ 10^{-10}$

simple calculations based on a ''quasi-two-dimensional'' adaptation of the equations of Rambaldi and Flierl (1983), whereby k^2 is replaced by $k^2 + l^2$, are given in Table A1.

The simple solution is found to underestimate the eddy enstrophy values obtained in the numerical model by as much as a factor of 2. Its qualitative agreement with the nonlinear model results is, however, not bad. More accurate estimates can be obtained by using a more realistic representation of the meridional flow structure. Using a limited number of modes, one has

$$\overline{U} = U_0 + \delta U[1 - \cos(2ly)], \quad \text{(A5)}$$

$$\Psi' = A \sin(kx) \sin(ly) + B \cos(kx) \sin(ly). \quad \text{(A6)}$$

Reformulating the original equations one obtains saturation values for the eddy enstrophy of 1.37 10^{-11} s^{-2}, 4.44 10^{-10} s^{-2}, 1.59 10^{-10} s^{-2}, and 3.09 10^{-10} s^{-2}, for $U_0 = 10$, 18, 33, and 46 m s^{-1} respectively, agreeing to within 20% with the model results. Introducing more degrees of freedom for the meridional structure can improve the agreement. However, for a qualitative understanding of the flow evolution, the results of the simple calculations seem sufficient. A calculation of a rigorous bound has little to add to our physical understanding and is of limited practical importance.

REFERENCES

Charney, J. G., and P. G. Drazin, 1961: Propagation of planetary-scale disturbances from the lower into the upper atmosphere. *J. Geophys. Res.,* **66,** 83–109.

——, and J. G. DeVore, 1979: Multiple flow equilibria in the atmosphere and blocking. *J. Atmos. Sci.,* **36,** 1205–1216.

Dickinson, R. E., 1969: Vertical propagation of planetary Rossby waves through an atmosphere with Newtonian cooling. *J. Geophys. Res.,* **74,** 929–938.

Dritschel, D. G., and R. Saravanan, 1994: Three-dimensional quasi-geostrophic contour dynamics, with an application to stratospheric vortex dynamics. *Quart. J. Roy. Meteor. Soc.,* **120,** 1267–1297.

Garcia, R. R., 1991: Parametrization of planetary wave breaking in the middle atmosphere. *J. Atmos. Sci.,* **48,** 1405–1419.

Haynes, P. H., 1985: Nonlinear instability of a Rossby-wave critical layer. *J. Fluid Mech.,* **161,** 493–511.

Juckes, M. N., and M. E. McIntyre, 1987: A high-resolution one-layer model of breaking planetary waves in the stratosphere. *Nature,* **328,** 590–596.

Karoly, D. J., and B. J. Hoskins, 1982: Three dimensional propagation of planetary waves. *J. Meteor. Soc. Japan,* **60,** 109–122.

Killworth, P. D., and M. E. McIntyre, 1985: Do Rossby-wave critical layers absorb, reflect, or over-reflect? *J. Fluid Mech.,* **161,** 449–492.

Lindzen, R. S., 1981: Turbulence and stress owing to gravity wave and tidal breakdown. *J. Geophys. Res.,* **86,** 9707–9714.

——, and M. R. Schoeberl, 1982: A note on the limits of Rossby wave amplitudes. *J. Atmos. Sci.,* **39,** 1171–1174.

——, B. Farrell, and D. Jacqmin, 1982: Vacillations due to wave interference: Applications to the atmosphere and to annulus experiments. *J. Atmos. Sci.,* **39,** 14–23.

McIntyre, M. E., and T. N. Palmer, 1983: Breaking planetary waves in the stratosphere. *Nature,* **305,** 593–600.

——, and ——, 1985: A note on the general concept of wave breaking for Rossby and gravity waves. *Pure Appl. Geophys.,* **123,** 964–975.

O'Neill, A., and V. D. Pope, 1988: Simulations of linear and nonlinear disturbances in the stratosphere. *Quart. J. Roy. Meteor. Soc.,* **114,** 1063–1110.

Polvani, L. M., and R. A. Plumb, 1992: Rossby wave breaking, microbreaking, filamentation, and secondary vortex formation: The dynamics of a perturbed vortex. *J. Atmos. Sci.,* **49,** 462–476.

——, D. W. Waugh, and R. A. Plumb, 1995: On the subtropical edge of the stratospheric surf zone. *J. Atmos. Sci.,* **52,** 1288–1309.

Rambaldi, S., and G. R. Flierl, 1983: Form drag instability and multible equilibria in the barotropic case. *Nuovo Cimento,* **6C,** 505–522.

Robinson, W. A., 1988: Irreversible wave-mean flow interactions in a mechanistic model of the stratosphere. *J. Atmos. Sci.,* **45,** 3413–3430.

Schoeberl, M. R., 1983: A study of stratospheric vacillations and sudden warmings on a β-plane. Part I: Single wave-mean flow interaction. *J. Atmos. Sci.,* **40,** 769–787.

Simmons, A. J., 1974: Planetary-scale disturbances in the polar winter stratosphere. *Quart. J. Roy. Meteor. Soc.,* **100,** 76–108.

Stewartson, K., 1978: The evolution of the critical layer of a Rossby wave. *Geophys. Astrophys. Fluid Dyn.,* **9,** 185–200.

Warn, T., and H. Warn, 1978: The evolution of a nonlinear critical level. *Stud. Appl. Math.,* **59,** 37–71.